



ELSEVIER

Available online at www.sciencedirect.com



International Journal of Thermal Sciences 42 (2003) 731–740

International
Journal of
Thermal
Sciences

www.elsevier.com/locate/ijts

Thermodynamic analysis of mixed convection in a channel with transverse hydromagnetic effect

Shohel Mahmud^a, Syeda Humaira Tasnim^b, Mohammad Arif Hasan Mamun^{b,*}

^a Department of Mechanical Engineering, Bangladesh University of Engineering and Technology, BUET, Dhaka 1000, Bangladesh

^b Department of Mechanical Engineering, University of Waterloo, 200 University Avenue West, Waterloo, ON Canada, N2L2G1

Received 13 February 2002; accepted 9 October 2002

Abstract

An analysis has been performed to study the First and Second laws (of thermodynamics) characteristics of flow and heat transfer inside a vertical channel made of two parallel plates under the action of transverse magnetic field. Combined free and forced convection inside the channel is considered. Flow is assumed to be steady, laminar, fully developed of electrically conducting, and heat-generating/absorbing fluid. Both vertical walls are kept isothermal at the same or different temperatures. Governing equations in Cartesian coordinates are first simplified and solved analytically to develop the expressions for velocity and temperature, entropy generation number (N_S), and irreversibility distribution ratio. Velocity, temperature, and entropy generation profiles are presented graphically. Full form of the governing equations are solved numerically using control-volume based finite volume method. Based on the numerical calculations, average entropy generation numbers are calculated for channels with different aspect ratios. Finally, a correlation is proposed which essentially expedite for calculating a geometric parameter (α_0) that will be characterized by minimum irreversibility at a particular value of Gr/Re (ratio of Grashof number and Reynolds number) and M (Hartmann number).

© 2003 Éditions scientifiques et médicales Elsevier SAS. All rights reserved.

Keywords: Entropy; Group parameter; Irreversibility; Magnetohydrodynamic; Mixed convection

1. Introduction

A combined free and forced convection flow of an electrically conducting and heat-generating/absorbing fluid in a channel in the presence of a transverse magnetic field is of special technical significance because of its frequent occurrence in many industrial applications such as geothermal reservoirs, cooling of nuclear reactors, thermal insulation, and petroleum reservoirs. This type of problem also arises in electronic packages, micro electronic devices during their operations.

In the absence of magnetic field, references [1–3] will give some ideas about fluid flow and thermal characteristics inside a vertical channel with symmetrical or asymmetrical thermal boundary condition. Sparrow and Cess [4] and Riley [5] studied buoyancy induced flow and transport in the

presence of magnetic field. Oreper and Szekely [6] analyzed the buoyancy driven flow in a rectangular cavity under the action of externally imposed magnetic field. Alboussiere et al. [7] did an asymptotic analysis to study the buoyancy driven convection in a uniform magnetic field. For closed geometry, Garandet et al. [8] studied the problem of free convective flow in a rectangular enclosure in the presence of transverse magnetic field. For rectangular vertical duct, Hunt [9] and Buhler [10] analyzed the fluid flow problem in magnetic field with or without buoyancy effect. For conducting fluid, Shercliff [11] analyzed the fluid flow characteristics in a pipe under transverse magnetic field. For an infinite vertical plate, Raptis and Kafoussias [12] studied the flow and heat transfer characteristics in the presence of porous medium and magnetic field. Later Raptis [13] extended the vertical plate problem to a vertical channel problem in the presence of magnetic field. For unsteady flow, Pan and Li [14] studied magnetohydrodynamic mixed convection in a vertical channel and Chamkha [15] reported the unsteady natural convection in a porous channel in the presence of magnetic field. For other geometry, Vajravelu

* Corresponding author.

E-mail addresses: mahmud_shohel@yahoo.com (S. Mahmud), shtasnime@engmail.uwaterloo.ca (S.H. Tasnim), mahmamun@engmail.uwaterloo.ca (M.A.H. Mamun).

Nomenclature

B_0	magnetic induction	$\text{Wb}\cdot\text{m}^{-2}$	X	dimensionless axial distance
C_P	specific heat	$\text{kJ}\cdot\text{kg}^{-1}\cdot\text{K}^{-1}$	y	transverse distance
Ec	Eckert number, $= v^2 \cdot Gr^2 \cdot w^{-2} \cdot C_p^{-1} \cdot \Delta T^{-1}$		Y	dimensionless transverse distance
g	gravitational acceleration	$\text{m}\cdot\text{s}^{-2}$	<i>Greek symbols</i>	
Gr	grashof number, $= g \cdot \beta \cdot \Delta T \cdot w^3 / \nu^2$		α	thermal diffusivity
k	thermal conductivity	$\text{W}\cdot\text{m}^{-1}\cdot\text{K}^{-1}$	α	aspect ratio, $= L/w$
M	Hartmann number, $= B_0 w \sqrt{\sigma / (\rho \nu)}$		β	thermal expansion coefficient
N_S	entropy generation number, $= \dot{S}''' / S_c'''$		ν	kinematic viscosity
N_{Sav}	average entropy generation number		ρ	fluid density
p	pressure	Pa	σ	fluid electrical conductivity
P	dimensionless pressure		Π_1	a constant, $= (Pr \times H)^{0.5}$
Pr	Prandtl number, $= \nu/\alpha$		Π_2	a constant
Q_0	dimensionless heat generation or absorption	$\text{W}\cdot\text{m}^{-3}\cdot\text{K}^{-1}$	Θ	dimensionless fluid temperature
\dot{S}'''	entropy generation rate	$\text{W}\cdot\text{m}^{-3}\cdot\text{K}^{-1}$	Φ	viscous work (see Eq. (21))
S_c'''	characteristic entropy transfer rate	$\text{W}\cdot\text{m}^{-3}\cdot\text{K}^{-1}$	Ψ	group parameter, $= (U_0^2 \mu T_0) / (\Delta T^2 k)$
T	temperature	$^\circ\text{C}$	<i>Subscript and superscript</i>	
u	fluid velocity in x direction	$\text{m}\cdot\text{s}^{-1}$	0	reference value
U	dimensionless axial velocity		L	value at left wall
v	fluid velocity in y direction	$\text{m}\cdot\text{s}^{-1}$	R	value at right wall
w	channel width	m	av	average value
x	axial distance	m	∞	ambient condition

and Nayfeh [16] and Chamkha [17] reported hydromagnetic free convection for cone and wedge without/with porous medium.

The above mentioned references that deal with free, forced, and mixed convection problems of different geometries in the presence and absence of magnetic field are very much restricted to first law (of thermodynamics) analysis in thermodynamic point of view. The contemporary trend in the field of heat transfer and thermal design is the second-law (of thermodynamics) analysis and its design-related concept of ‘Entropy Generation Minimization’ (see Bejan [18,19]). This new trend is important and, at the same time, necessary, if the heat transfer community is to contribute to a viable engineering solution to the energy problems. Entropy generation is associated with thermodynamic irreversibility, which is common in all types of heat transfer processes. Different sources are responsible for generation of entropy like heat transfer down temperature gradient, characteristic of convective heat transfer, viscous effect etc. Bejan [19] focused on the different reasons behind entropy generation in applied thermal engineering. Generation of entropy destroys available work of a system. Therefore, it makes good engineering sense to focus on irreversibility (see Bejan [18,19]) of heat transfer and fluid flow processes and try to understand the function of entropy generation mechanism. Bejan [20] first presented the second-law aspect of heat transfer using different examples of fundamental forced convection problems. He introduced the concept of entropy generation num-

ber, irreversibility distribution ratio and presented the spatial distribution of irreversibility, entropy generation profiles or maps for the example problems. Since then, numerous investigations have been performed to determine the entropy generation and irreversibility profiles for different geometric configurations, flow situations and thermal boundary conditions. Most of them are numerical calculations due to non-linear nature of flow governing equations. Very few of them are done considering analytical approach of solution. For a good review, the second law analysis as well as entropy generation profiles are available in the references by Bejan [19, 20] and Drost and Zaworski [21].

The purpose of this article is to analyze the first and second laws (of thermodynamics) characteristics of fully developed mixed convection flow in a channel in the presence of heat generation/absorption and transverse hydromagnetic effect with isothermal boundary condition. Expressions for dimensionless velocity and temperature, entropy generation number derived.

2. Problem formulation

Consider fully developed, laminar, steady mixed convection flow of an electrically conducting and heat-generating/absorbing fluid in a vertical channel in the presence of a transverse magnetic field applied normal to the flow direction as shown in Fig. 1. The fluid is assumed to be incompressible with constant properties except the density in the

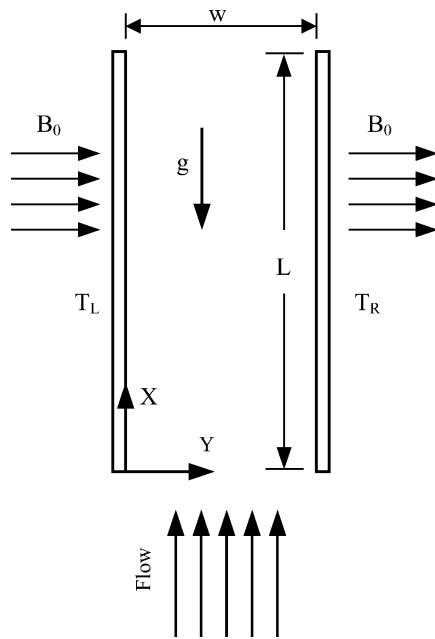


Fig. 1. Schematic diagram of the problem under consideration.

buoyancy term in the x -momentum equation. The magnetic Reynolds number is assumed to be small, so that the induced magnetic field is neglected and the Hall effect of magnetohydrodynamics is assumed to be negligible. The governing equations for this investigation are based on the usual balance laws of mass, momentum, and energy modified to account for buoyancy effects, and hydromagnetic and heat generation/absorption effects. The governing equations are as follows:

Continuity:

$$\frac{\partial u}{\partial x} + \frac{\partial v}{\partial y} = 0 \tag{1}$$

x -momentum:

$$u \frac{\partial u}{\partial x} + v \frac{\partial u}{\partial y} = -\frac{1}{\rho} \frac{\partial p}{\partial x} + g\beta(T - T_m) + \nu \left[\frac{\partial^2 u}{\partial x^2} + \frac{\partial^2 u}{\partial y^2} \right] - \frac{\sigma B_0^2}{\rho} u \tag{2}$$

y -momentum:

$$u \frac{\partial v}{\partial x} + v \frac{\partial v}{\partial y} = -\frac{1}{\rho} \frac{\partial p}{\partial y} + \nu \left[\frac{\partial^2 v}{\partial x^2} + \frac{\partial^2 v}{\partial y^2} \right] \tag{3}$$

Energy:

$$u \frac{\partial T}{\partial x} + v \frac{\partial T}{\partial y} = \alpha \left[\frac{\partial^2 T}{\partial x^2} + \frac{\partial^2 T}{\partial y^2} \right] \pm \frac{Q_0}{\rho c_p} (T - T_m) + \frac{\sigma B_0^2}{\rho c_p} u^2 \tag{4}$$

In Eqs. (1)–(4), ν , ρ , α , σ , Q_0 , and B_0 stand for kinematic viscosity, fluid density, thermal diffusivity, electrical conductivity of the fluid, heat generation/absorption parameter, and magnetic induction respectively. Eqs. (1)–(4) are put

into their dimensionless forms using appropriate scaling parameters. Axial and transverse distances (x and y) are scaled with channel width w . Velocity u and v are scaled with the inlet velocity u_0 . Dimensionless temperature Θ is defined as $(T - T_m)/(T_R - T_m)$ where T_m is the mean temperature and will be defined later. Other dimensionless parameters are defined in nomenclature. The dimensionless forms of Eqs. (1)–(4) become

$$\frac{\partial U}{\partial X} + \frac{\partial U}{\partial Y} = 0 \tag{5}$$

$$U \frac{\partial U}{\partial X} + V \frac{\partial U}{\partial Y} = -\frac{\partial P}{\partial X} + \frac{Gr}{Re^2} \Theta + \frac{1}{Re} \left[\frac{\partial^2 U}{\partial X^2} + \frac{\partial^2 U}{\partial Y^2} \right] - \frac{M^2}{Re} U \tag{6}$$

$$U \frac{\partial V}{\partial X} + V \frac{\partial V}{\partial Y} = -\frac{\partial P}{\partial Y} + \frac{1}{Re} \left[\frac{\partial^2 V}{\partial X^2} + \frac{\partial^2 V}{\partial Y^2} \right] \tag{7}$$

$$U \frac{\partial \Theta}{\partial X} + V \frac{\partial \Theta}{\partial Y} = \frac{1}{Re Pr} \left[\frac{\partial^2 \Theta}{\partial X^2} + \frac{\partial^2 \Theta}{\partial Y^2} \right] \pm \frac{H}{Re} \Theta + \frac{EcM^2}{Re} U^2 \tag{8}$$

subjected to the following boundary conditions

$$\begin{aligned} 0 \leq X \leq \lambda \quad \text{and} \quad Y = 0: \quad U = V = 0 \quad \text{and} \quad \Theta = \Theta_L \\ 0 \leq X \leq \lambda \quad \text{and} \quad Y = 1: \quad U = V = 0 \quad \text{and} \quad \Theta = \Theta_R \\ 0 \leq Y \leq 1 \quad \text{and} \quad X = 0: \quad U = U_0 \\ V = 0, \quad \text{and} \quad \Theta = \Theta_0 \\ 0 \leq Y \leq 1 \quad \text{and} \quad X = \lambda: \quad \frac{\partial U}{\partial X} = \frac{\partial V}{\partial X} = \frac{\partial \Theta}{\partial X} = 0 \end{aligned} \tag{9}$$

3. Analytical solution

To get the expressions for velocity and temperature in dimensionless forms, Eqs. (5)–(8) should be solved. However, Eqs. (5)–(8) are nonlinear in nature and coupled by the temperature Θ . It is difficult to get an analytical solution unless they are simplified to linear forms. Assuming a hydrodynamically and thermally fully developed flow and neglecting the transverse velocity $V (V \ll U)$, Eq. (5) gives $\partial U/\partial X = 0$. Based on these assumptions, Eq. (6) is simplified to the following form

$$\frac{\partial^2 U}{\partial Y^2} - M^2 U = \frac{\partial P^*}{\partial X} - \frac{Gr}{Re} \Theta \tag{10}$$

where modified pressure P^* is the product of P and Re . If the fluid temperature gradient along the axial distance X is neglected, that is, the fluid temperature is uniform along the X direction, as is the case for the isothermal boundary condition, and if the magnetic dissipation effect is neglected, analytical solutions to the governing equations are possible. Setting $Ec = 0$ and $\partial \Theta/\partial X = 0$ in Eq. (8), we get

$$\frac{\partial^2 \Theta}{\partial Y^2} \pm Pr H \Theta = 0 \tag{11}$$

It should be mentioned that the form of the analytical solution for Θ is different for a heat-generating fluid (positive sign in Eq. (11)) than for a heat-absorbing fluid (negative sign in Eq. (11)).

4. Heat-generating fluid

For this type of fluid the energy equation (Eq. (11)) with the positive sign in the second term is a linear differential equation. Introducing two constant parameters, $\Pi_1 = (Pr \times H)^{0.5}$ and $\Pi_2 = M$, the following equations is the closed-form solution of Eq. (11) for Θ :

$$\Theta = C_1 \cos(\Pi_1 Y) + C_2 \sin(\Pi_1 Y) \quad (12)$$

where C_1 and C_2 are two arbitrary constants determined by the thermal boundary conditions given in Eq. (9). Using the boundary conditions, C_1 and C_2 becomes

$$\begin{aligned} C_1 &= \Theta_L \\ C_2 &= \frac{\Theta_R - \Theta_L \cos(\Pi_1)}{\sin(\Pi_1)} \end{aligned} \quad (13)$$

With the solution for Θ already determined, Eq. (10) can be solved for velocity U subjected to the no-slip boundary conditions given in Eq. (9). Avoiding detail arithmetic operations, the expression for dimensionless velocity U becomes

$$\begin{aligned} U &= C_3 + C_4 \cos(\Pi_1 Y) + C_5 \sin(\Pi_1 Y) \\ &+ C_6 \cosh(\Pi_2 Y) + C_7 \sinh(\Pi_2 Y) \end{aligned} \quad (14)$$

In the above equation, the constants C_3 , C_4 , C_5 , C_6 , and C_7 can be defined as

$$\begin{aligned} C_3 &= -\frac{\partial P / \partial X}{\Pi_2^2}, & C_4 &= \frac{Gr}{Re} \frac{C_1}{\Pi_1^2 + \Pi_2^2} \\ C_5 &= \frac{Gr}{Re} \frac{C_2}{\Pi_1^2 + \Pi_2^2}, & C_6 &= -C_3 - C_4 \\ C_7 &= \frac{C_6 \cosh(\Pi_2) + C_3 + C_4 \cos(\Pi_1) + C_5 \sin(\Pi_1)}{-\sinh(\Pi_2)} \end{aligned} \quad (15)$$

Dimensionless form of average velocity (U_{av}) through the channel is

$$\begin{aligned} U_{av} &= C_3 + \frac{C_4 \sin(\Pi_1) - C_5 [\cos(\Pi_1) - 1]}{\Pi_1} \\ &+ \frac{C_6 \sinh(\Pi_2) + C_7 [\cosh(\Pi_2) - 1]}{\Pi_2} \end{aligned} \quad (16)$$

5. Heat-absorbing fluid

For this type of fluid, the energy equation (Eq. (11)) with the negative sign in the second term is a linear differential equation that has the following closed-form solution for Θ

$$\Theta = D_1 \cosh(\Pi_1 Y) + D_2 \sinh(\Pi_1 Y) \quad (17)$$

where D_1 and D_2 are arbitrary constants determined by the thermal boundary conditions. Using the boundary conditions, D_1 and D_2 becomes

$$\begin{aligned} D_1 &= \Theta_L \\ D_2 &= \frac{\Theta_R - \Theta_L \cosh(\Pi_1)}{\sinh(\Pi_1)} \end{aligned} \quad (18)$$

With the solution for Θ already determined Eq. (10) can be solved for velocity U subjected to the no-slip boundary conditions given in Eq. (9). Avoiding detail arithmetic operations, the expression for dimensionless velocity U becomes:

$$\begin{aligned} U &= D_3 + D_4 \cosh(\Pi_1 Y) + D_5 \sinh(\Pi_1 Y) \\ &+ D_6 \cosh(\Pi_2 Y) + D_7 \sinh(\Pi_2 Y) \end{aligned} \quad (19)$$

In the above equation, the constants D_3 , D_4 , D_5 , D_6 , and D_7 can be defined as:

$$\begin{aligned} D_3 &= -\frac{\partial P / \partial X}{\Pi_2^2}, & D_4 &= -\frac{Gr}{Re} \frac{D_1}{\Pi_1^2 - \Pi_2^2} \\ D_5 &= -\frac{Gr}{Re} \frac{D_2}{\Pi_1^2 - \Pi_2^2}, & D_6 &= -D_3 - D_4 \\ D_7 &= \frac{D_6 \cosh(\Pi_2) + D_3 + D_4 \cosh(\Pi_1) + D_5 \sinh(\Pi_1)}{-\sinh(\Pi_2)} \end{aligned} \quad (20)$$

Dimensionless form of average velocity (U_{av}) through the channel is

$$\begin{aligned} U_{av} &= D_3 + \frac{D_4 \sinh(\Pi_1) - D_5 [\cosh(\Pi_1) - 1]}{\Pi_1} \\ &+ \frac{D_6 \sinh(\Pi_2) + D_7 [\cosh(\Pi_2) - 1]}{\Pi_2} \end{aligned} \quad (21)$$

6. Second law analysis

The foundation of knowledge of entropy production goes back to Clausius and Kelvin's studies on the irreversible aspects of the Second Law of Thermodynamics. Since then the theories based on these foundations have rapidly developed. However, the entropy production resulting from temperature differences has remained untreated by classical thermodynamic, which motivates many researchers to conduct analyses of fundamental and applied engineering problems based on Second law analysis. Review of such analyses is beyond the scope of this paper. For a comprehensive reference, see Bejan [19].

Convection process in a channel is inherently irreversible. The non-equilibrium conditions due to the exchange of energy and momentum, within the fluid and at the solid boundaries, cause a continuous entropy generation. One part of this entropy production is due to the transfer of heat in the direction of finite temperature gradients, which is common almost in all types thermal engineering applications (see Bejan [19] and Bejan et al. [22]). This temperature entropy production rate can be evaluated from the first term at the

right-hand side of Eq. (22). Another part of the entropy production arises due to the fluid friction and in general termed as the fluid friction irreversibility, which is calculated using the second term at the right-hand side of Eq. (22). The magnetic effect introduces an additional work due to the magnetic field and magnetization. Irreversibility due to magnetic effect can be calculated from the third term. The general equation for entropy generation (Woods [23])

$$\dot{S}''' = \frac{k}{T_0^2} [\nabla T]^2 + \frac{\mu}{T_0} \Phi + \frac{1}{T_0} [(\mathbf{J} - \mathbf{QV}) \cdot (\mathbf{E} + \mathbf{V} \times \mathbf{B})] \quad (22)$$

where \mathbf{J} , \mathbf{Q} , \mathbf{V} , \mathbf{E} , \mathbf{V} , \mathbf{B} , and T_0 are electric current, electric charge density, velocity vector, electric field, magnetic induction and reference temperature and for present problem $T_0 = T_m$. In Eq. (22), the terms Φ and \mathbf{J} at the right-hand side are

$$\Phi = 2 \left[\left(\frac{\partial u}{\partial x} \right)^2 + \left(\frac{\partial v}{\partial y} \right)^2 + \left(\frac{\partial w}{\partial z} \right)^2 \right] - \frac{2}{3} [\text{div}(\mathbf{V})]^2 + \left(\frac{\partial u}{\partial y} + \frac{\partial v}{\partial x} \right)^2 + \left(\frac{\partial v}{\partial z} + \frac{\partial w}{\partial y} \right)^2 + \left(\frac{\partial w}{\partial x} + \frac{\partial u}{\partial z} \right)^2 \quad (23)$$

$$\mathbf{J} = \sigma(\mathbf{E} + \mathbf{V} \times \mathbf{B})$$

For present problem, Eq. (22) can be simplified into the following form

$$\dot{S}''' = \frac{k}{T_0^2} \left[\frac{\partial T}{\partial y} \right]^2 + \frac{\mu}{T_0} \left[\frac{\partial u}{\partial y} \right]^2 + \frac{\sigma B_0^2}{T_0} u^2 \quad (24)$$

Entropy generation rate is positive and finite as long as temperature and velocity gradients are present in the medium. The dimensionless form of entropy generation rate is the entropy generation number (N_S) and is equal to the ratio of actual entropy generation rate to the characteristic entropy transfer rate [20]. The characteristic entropy transfer rate for the channel with isothermal boundary condition is

$$\dot{S}_c''' = \left[\frac{k(\Delta T)^2}{w^2 T_0^2} \right] \quad (25)$$

When non-dimensionized using the same parameters already used for scaling purpose, Eq. (22) becomes

$$N_S = \left[\frac{\partial \Theta}{\partial Y} \right]^2 + \Psi \left[\frac{\partial U}{\partial Y} \right]^2 + \Psi M^2 U^2 \quad (26)$$

In the above equation, the group parameter Ψ is equal to $(U_0^2 \mu T_0) / (\Delta T^2 k)$. Using Eqs. (12), (14), and (26), the expression for entropy generation number for heat-generating fluid becomes

$$N_S = \Pi_1^2 [C_1 \sin(\Pi_1 Y) - C_2 \cos(\Pi_1 Y)]^2 + \Psi [\Pi_1 \{-C_4 \sin(\Pi_1 Y) + C_5 \cos(\Pi_1 Y)\}]$$

$$+ \Pi_2 \{C_6 \sinh(\Pi_2 Y) + C_7 \cosh(\Pi_2 Y)\}^2 + \Psi M^2 U^2 \quad (27)$$

Using Eqs. (17), (19), and (26), the expression for entropy generation number for heat-absorbing fluid becomes

$$N_S = \Pi_1^2 [D_1 \sinh(\Pi_1 Y) + D_2 \cosh(\Pi_1 Y)]^2 + \Psi [\Pi_1 \{D_4 \sin(\Pi_1 Y) + D_5 \cos(\Pi_1 Y)\} + \Pi_2 \{D_6 \sinh(\Pi_2 Y) + D_7 \cosh(\Pi_2 Y)\}]^2 + \Psi M^2 U^2 \quad (28)$$

7. Results and discussions

It is difficult to study the influence of all parameters involved in the present problem on the flow and thermal field along with entropy generation characteristics. Therefore, a selected set of graphical results is presented in Figs. 2–12 that will give a good understanding of the influence of different parameters on the velocity, temperature, and entropy generation profiles. Both symmetrical ($\Theta_L = 1$, $\Theta_R = 1$) and asymmetrical temperature ($\Theta_L = 0$, $\Theta_R = 1$) at the walls are considered for the heat generating fluid.

Modified dimensionless velocity (U^*) is calculated by dividing the velocity U by the average velocity U_{av} . Fig. 2 shows the variation of U^* as a function of Y at different Hartmann numbers (M), ranging 0–30, associated with the case of constant and symmetrical wall temperatures. Velocity profiles are symmetrical about the centerline ($Y = 0.5$) of the channel for each value of M . Increase in the values of M have a tendency to slow down the movement of the fluid in the channel. This is because the application of magnetic field creates a resistive force similar to the drag force that acts in the opposite direction of the fluid

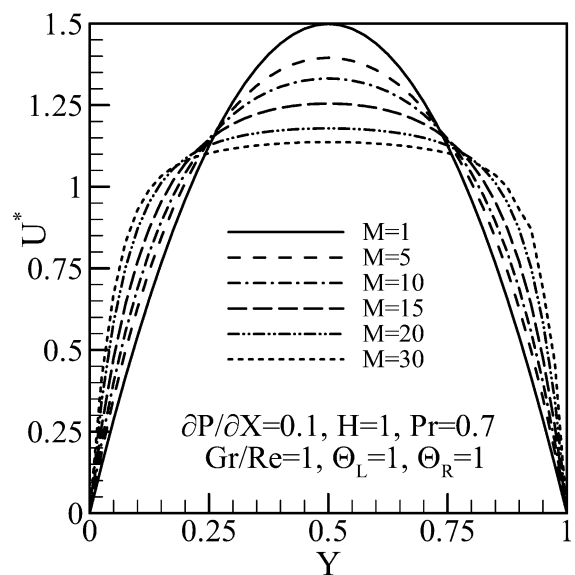


Fig. 2. Velocity U^* as a function of Y at different M for symmetric temperature at the boundary.

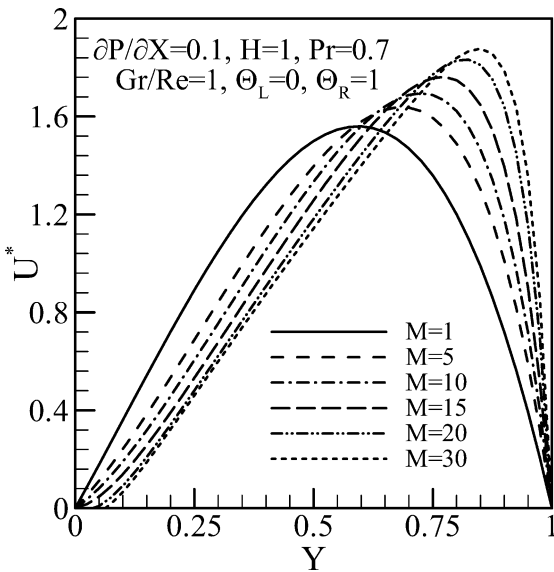


Fig. 3. Velocity U^* as a function of Y at different M for asymmetric temperature at the boundary.

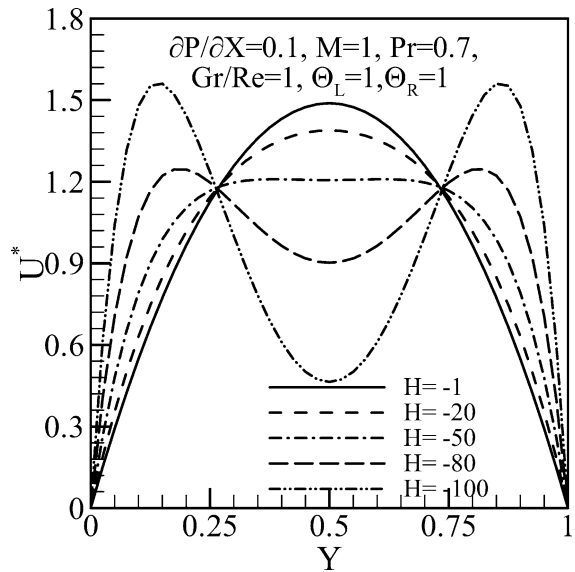


Fig. 5. Velocity U^* as a function of Y at different negative H for symmetric temperature at the boundary.

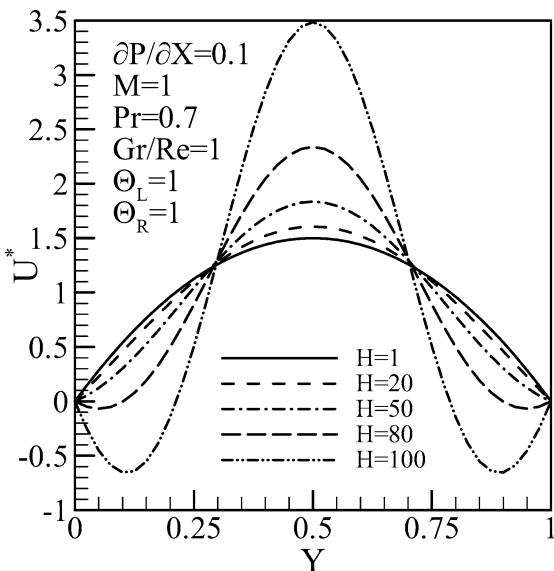


Fig. 4. Velocity U^* as a function of Y at different positive H for symmetric temperature at the boundary.

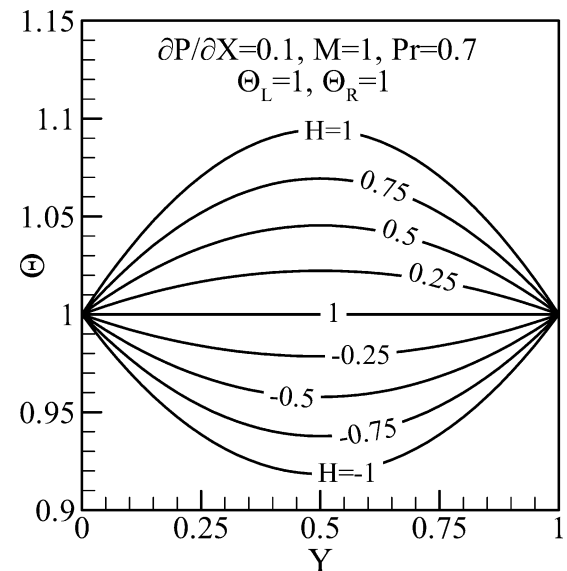


Fig. 6. Temperature Θ as a function of Y at different H for symmetric temperature at the boundary.

motion, thus causing the velocity of the fluid to decrease. This is depicted in the decreases of the U^* as M increases in Fig. 2. Velocity becomes maximum at the centerline of the channel resulting zero velocity gradient ($\partial U/\partial Y$) for each velocity profile. Fig. 3 shows the influence of asymmetric temperature at the walls on the velocity profiles keeping all other variables same as in Fig. 2. In this case, velocity profiles are not symmetric about the centerline of the channel. Asymmetry increases more so as M increases. Maximum velocity (as well as zero velocity gradient) moves towards the hot wall (in this case right wall) as M increases.

For constant and symmetric wall temperatures, the effect of the heat-generation or absorption coefficient (H) on

velocity profiles is shown in Fig. 4 for the heat generation case (positive H) and in Fig. 5 for the heat absorption case (negative H). Velocity profiles are symmetrical about the centerline ($Y = 0.5$) of the channel. Increase in the values of H causes warming the fluid in the channel, which increases the buoyancy effect. Two distinct zones are observed in Fig. 4. For $0.3 \leq Y \leq 0.7$, increasing tendency of the fluid velocity is observed with increasing H . For $Y < 0.3$ and $Y > 0.7$, the fluid motion is retarded with increasing H . Flow reversal is observed at high H near the walls. Magnitude of reverse velocity is small at $H = 80$, which is high in magnitude at $H = 100$. For the heat absorption case (negative H), the fluid motion shows

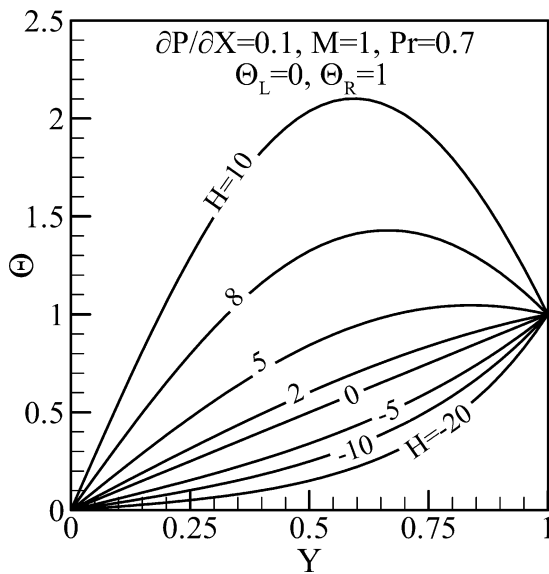


Fig. 7. Temperature Θ as a function of Y at different H for asymmetric temperature at the boundary.

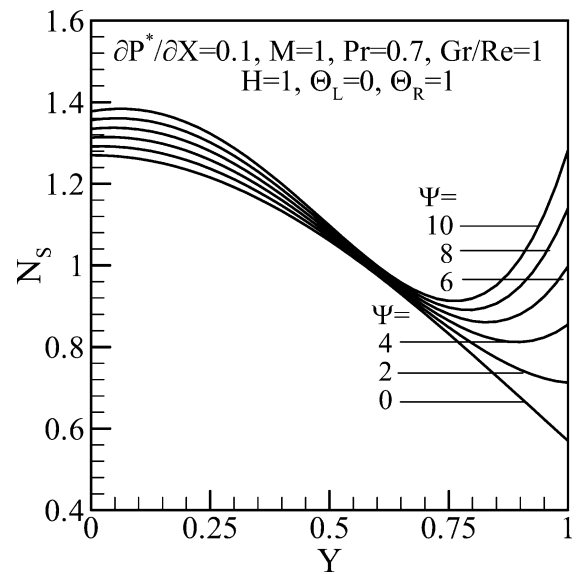


Fig. 9. Entropy generation number N_S as a function of Y at different Ψ for asymmetric temperature at the boundary.

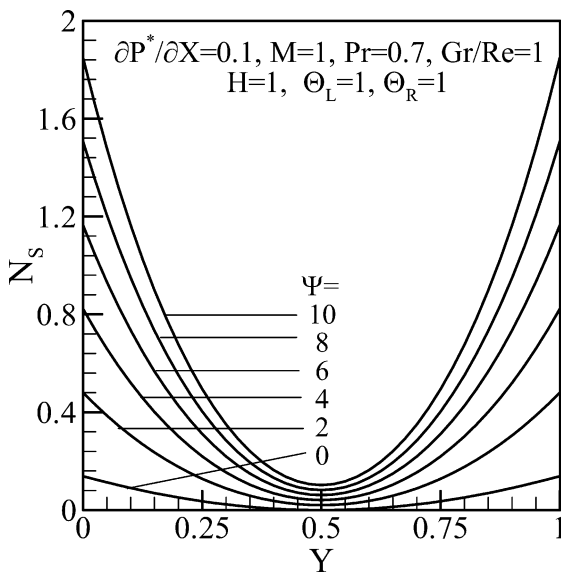


Fig. 8. Entropy generation number N_S as a function of Y at different Ψ for symmetric temperature at the boundary.

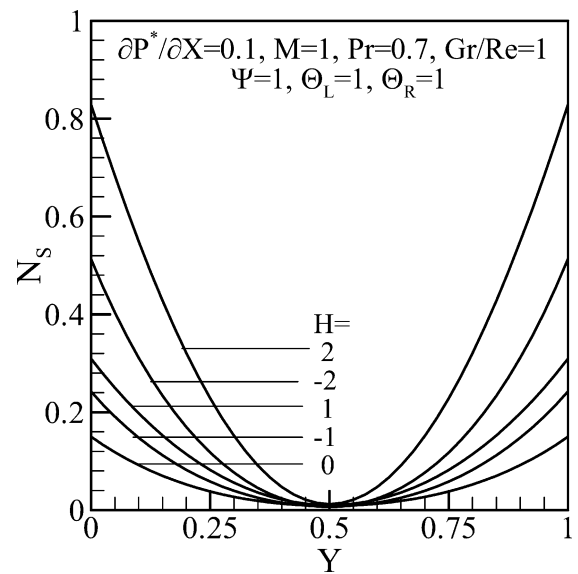


Fig. 10. Entropy generation number N_S as a function of Y at different H for symmetric temperature at the boundary.

retardation (see Fig. 5) around the channel centerline ($0.3 \leq Y \leq 0.7$) for increasing $|H|$. For $Y < 0.3$ and $Y > 0.7$, magnitude of the velocity is higher for higher $|H|$.

Figs. 6 and 7 show the influence of the heat-generation or absorption parameter (H) on fluid temperature profiles for the cases of symmetric and asymmetric temperatures at the walls respectively keeping other parameters constant as shown in figures. The positive value of H corresponds heating, while the negative value corresponds cooling of the fluid. For $H = 0$, no heat generates and the corresponding temperature profile becomes straight line (for symmetrical case) and linear (for asymmetrical case) as shown in Figs. 6 and 7. For the symmetry of the thermal boundary

condition, temperature profiles are symmetrical about the centerline of the channel (see Fig. 6). Temperature is minimum at the centerline of the channel for $H < 0$, while temperature is maximum for $H > 0$. As expected, increasing H causes the fluid to become warmer and therefore increase its temperature. Because of non-symmetric thermal boundary condition, temperature profiles are asymmetric (see Fig. 7).

For constant and symmetrical wall temperatures, entropy generation number (N_S) is plotted as a function of Y in Fig. 8 at different group parameters (Ψ). The group parameter determines the relative importance of viscous effect (see Bejan [19]). For all Ψ , entropy generation

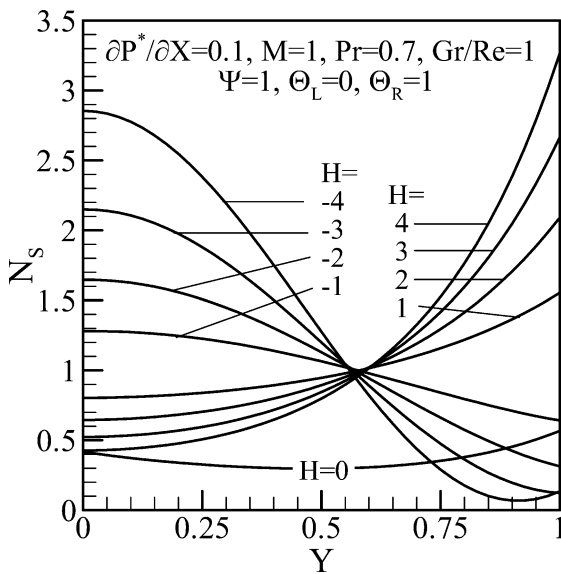


Fig. 11. Entropy generation number N_S as a function of Y at different H for asymmetric temperature at the boundary.

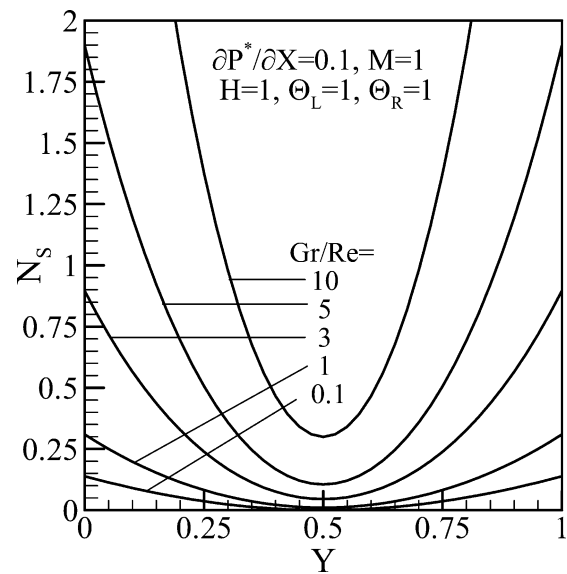


Fig. 13. Entropy generation number N_S as a function of Y at different Gr/Re for symmetric temperature at the boundary.

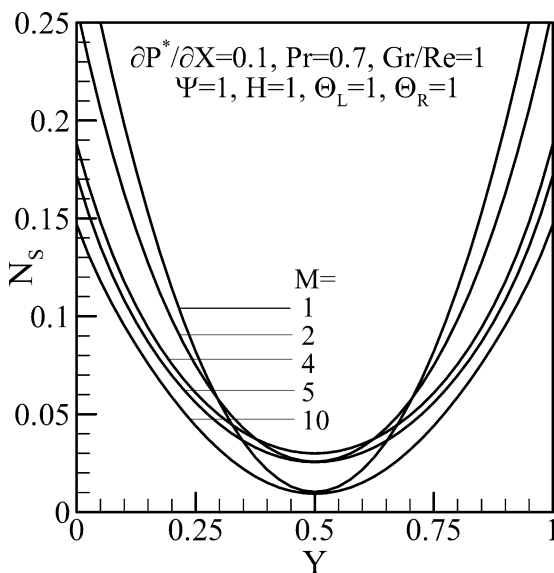


Fig. 12. Entropy generation number N_S as a function of Y at different M for symmetric temperature at the boundary.

rate is minimum at the centerline of the channel. Both velocity and temperature are maximum (or minimum) at the centerline (see Figs. 2 and 6), which cause zero velocity and temperature gradients ($\partial U/\partial Y$ and $\partial T/\partial Y$) leaving no contribution to the entropy generation from the gradient terms of entropy generation equation (first and second terms of Eq. (24)). N_S profiles are symmetrical about the centerline of the channel. For a particular Y , N_S increases with the increase of Ψ . Both walls act as a strong concentrator of irreversibility where N_S is maximum.

Fig. 9 shows the entropy generation profiles for asymmetric thermal boundary condition. For all Ψ , left wall acts as a strong concentrator of irreversibility. Magnitude of the

difference between two consecutive N_S profiles decreases along Y . N_S profiles merge with each other at $Y = 0.6$. After this point ($Y = 0.6$), N_S profiles show different characteristics depending on the value of Ψ . For $\Psi = 0$, fluid friction irreversibility becomes zero and entropy generation number falls linearly towards the hot wall. For higher Ψ (e.g., $\Psi = 8$), fluid friction irreversibility dominates and entropy generation number rapidly increases with Y .

The influence of heat-generation or absorption parameter (H) on entropy generation number is presented in Fig. 10 for the symmetric, and in Fig. 11 for the asymmetric thermal boundary conditions. For the symmetric case (see Fig. 10), entropy generation distribution is still characterized by nice concave shaped profile. Heat transfer has no contribution to entropy generation at $H = 0$ ($\partial T/\partial Y = 0$ everywhere, see Fig. 6), showing minimum entropy generation rate (compared to the profiles of other H). Heating of the fluid (positive H) shows higher entropy generation rate than the cooling of the fluid (negative H). At a particular Y , entropy generation rate is higher for higher value of H (absolute value). This scenario becomes complicated for asymmetric thermal boundary condition (see Fig. 11) due to the complex nature of velocity and temperature distribution patterns. For all H , profiles intersect approximately at $Y \approx 0.6$. For $Y < 0.6$, entropy generation rate is higher for lower value of H and opposite scenario is observed for $Y > 0.425$.

Influence of Hartmann number (M) on the entropy generation profile is shown in Fig. 12. The parameter M is not too much dominating on entropy generation. A large variation of M causes a small variation in the rate of entropy generation. Fig. 13 shows the influence of Gr/Re on the local entropy generation rate.

8. Numerical calculation

To conduct a numerical analysis we used the technique similar as Hortmann et al. [24] based on the Finite-volume method as described in Ferziger and Peric [25]. The solution domain is first subdivided into finite number of control volumes (CV). Body fitted, non-orthogonal grids are oriented in such a way that the number of CV is higher near the walls. All variables are calculated at the center of each CV (non-staggered scheme). SIMPLE algorithm is used. Stone’s SIP solver [25] is used to solve the system of discretized equations. Details about numerical calculation are avoided.

For a particular Gr/Re and M , field values of u -velocity, v -velocity, and temperature are calculated numerically using Eqs. (5)–(8). Then using Eq. (22), local values of entropy

generation numbers (N_S) are calculated and then integrated over the volume of the channel (\forall) to get the volume averaged entropy generation number (N_{Sav}) as follows:

$$N_{Sav} = \int_{\forall} N_S d\forall = \int_{X=0}^{X=1} \int_{Y=0}^{Y=\alpha} \int_{Z=0}^{Z=1} N_S dX dY dZ \quad (29)$$

For a range of aspect ratio (α) of the channel, there exists a particular value of α ($= \alpha_0$) where entropy generation (irreversibility) become minimum. The corresponding value of minimum entropy generation is symbolically expressed as $N_{Sav,min}$, which is a function of Gr/Re and M . For numerical calculation, internal heat generation and/or absorption is assumed to be negligible.

Fig. 14 shows the distribution of $N_{Sav}/N_{Sav,min}$ as a function of α at different Gr/Re for a particular value of Hartmann number (M). For a particular Gr/Re , average entropy generation decreases with an increasing α , shows its minimum at particular value of α ($= \alpha_0$), then increases with further increase of α . The geometric parameter, α_0 , is plotted in Fig. 15 as a function of Gr/Re at different Hartmann number. The linear nature of the $\alpha_0 - Gr/Re$ profiles in logarithmic plot enable us to construct a correlation in the following form:

$$\alpha_0 = 6.32581 \times (M)^{0.223384} \times \left(\frac{Gr}{Re}\right)^{-0.11779} \quad (0.1 \leq M \leq 10 \text{ and } 0.1 \leq Gr/Re \leq 10) \quad (30)$$

The above correlation shows good agreement with the numerical calculations within $\pm 5\%$ accuracy.

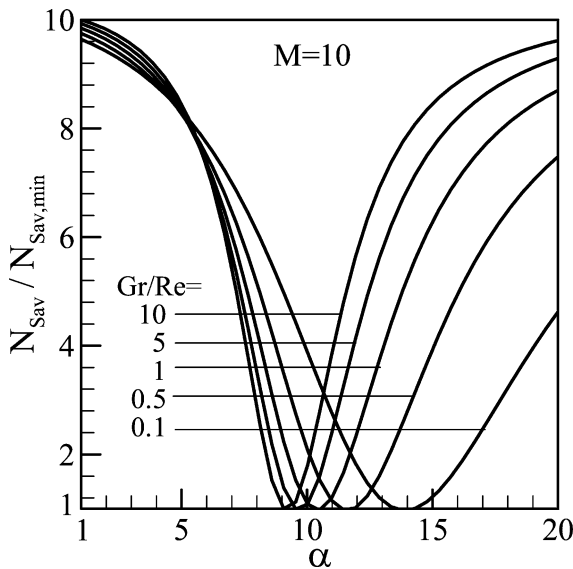


Fig. 14. Average entropy generation number at different Gr/Re .

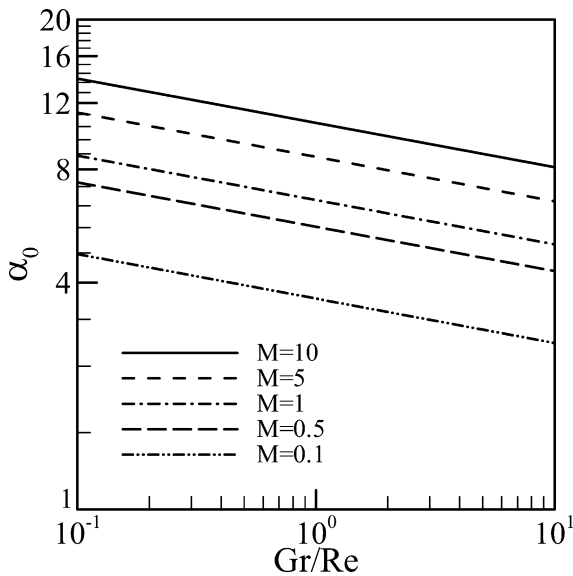


Fig. 15. Distribution of α_0 as a function of Gr/Re at different M .

9. Conclusion

Analytical expressions have been developed for velocity, temperature, and entropy generation number for mixed convection flow in a vertical channel under the action of transverse magnetic field. Only isothermal boundary condition is considered with symmetric and asymmetric temperatures at the walls. With symmetrical temperature at the walls, profiles for velocity, temperature and entropy generation number show symmetrical nature. Symmetry of these profiles is distorted for asymmetrical thermal boundary condition. Both walls act as strong concentrator of irreversibility due to high velocity and temperature gradients. Group parameters have significant effect on entropy generation rate. Higher value of group parameter causes higher entropy generation. For positive value of heat generation/absorption parameter, entropy generation rate is higher than the negative value of same magnitude. Based on the numerical calculation, a correlation is proposed which can calculate a geometric parameter (α_0) at which value irreversibility is minimum.

References

- [1] S. Habchi, S. Acharya, Laminar mixed convection in a symmetrically or asymmetrically heated vertical channel, *Numer. Heat Transfer* 9 (1986) 605–618.
- [2] W. Aung, G. Worku, Developing flow and flow reversal in a vertical channel with asymmetric wall temperatures, *J. Heat Transfer* 108 (1986) 299–304.
- [3] M. Iqbal, B.D. Aggarwala, A.G. Fowler, Laminar combined free and forced convection in vertical non-circular ducts under uniform heat flux, *Internat. J. Heat Mass Transfer* 12 (1969) 1123–1139.
- [4] E.M. Sparrow, R.D. Cess, Effect of magnetic field on free convection heat transfer, *Internat. J. Heat Mass Transfer* 3 (1961) 267–274.
- [5] N. Riley, Magnetohydrodynamics free convection, *J. Fluid Mech.* 18 (1964) 577–586.
- [6] G.M. Oreper, J. Szekely, The effect of an external imposed magnetic field on buoyancy driven flow in a rectangular cavity, *J. Crystal Growth* 64 (1983) 505–515.
- [7] T. Alboussiere, J.P. Garandet, R. Moreau, Buoyancy-driven convection with a uniform magnetic field, Part 1. Asymptotic analysis, *J. Fluid Mech.* 253 (1983) 545–563.
- [8] J.P. Garandet, T. Alboussiere, R. Moreau, Buoyancy driven convection in a rectangular enclosure with a transverse magnetic field, *Internat. J. Heat Mass Transfer* 35 (1992) 741–749.
- [9] J.C.R. Hunt, Magnetohydrodynamic flow in a rectangular duct, *J. Fluid Mech.* 21 (1965) 577–590.
- [10] L. Buhler, Laminar buoyant magnetohydrodynamic flow in a rectangular duct, *Phys. Fluids* 10 (1998) 223–236.
- [11] J.A. Shercliff, Steady motion of conducting fluids in pipes under transverse magnetic fields, *Proc. Cambridge Philos. Soc.* 49 (1953) 136–144.
- [12] A. Raptis, N. Kafoussias, Heat transfer in flow through a porous medium bounded by an infinite vertical plane under the action of magnetic field, *Energy Res.* 6 (1982) 241–245.
- [13] A. Raptis, Flow through porous medium in the presence of a magnetic field, *Energy Res.* 10 (1986) 97–100.
- [14] B. Pan, B.Q. Li, Effect of magnetic fields on oscillating mixed convection, *Internat. J. Heat Mass Transfer* 41 (1998) 2705–2710.
- [15] A.J. Chamkha, Unsteady hydromagnetic natural convection in a fluid-saturated porous medium channel, *Adv. Filtration Separation Tech.* 10 (1996) 369–375.
- [16] K. Vajravelu, J. Nayfeh, Hydromagnetic convection at a cone and a wedge, *Internat. Commun. Heat Mass Transfer* 19 (1992) 701–710.
- [17] A.J. Chamkha, Non-Darcy hydromagnetic free convection from a cone and a wedge in porous media, *Internat. Commun. Heat Mass Transfer* 23 (1996) 875–887.
- [18] A. Bejan, Second-law analysis in heat transfer and thermal design, *Adv. Heat Transfer* 15 (1982) 1–58.
- [19] A. Bejan, *Entropy Generation Minimization*, CRC Press, Boca Raton, NY, 1996.
- [20] A. Bejan, A study of entropy generation in fundamental convective heat transfer, *J. Heat Transfer* 101 (1979) 718–725.
- [21] M.K. Drost, J.R. Zaworski, A review of second law analysis techniques applicable to basic thermal science research, *ASME AES* 4 (1988) 7–12.
- [22] A. Bejan, G. Tsatsaronis, M. Moran, *Thermal Design and Optimization*, Wiley, New York, 1996.
- [23] L.C. Woods, *The Thermodynamics of Fluid Systems*, Oxford University Press, Oxford, 1975.
- [24] M. Hortmann, M. Peric, G. Scheuerer, Finite volume multigrid prediction of laminar natural convection: Bench-mark solutions, *Internat. J. Numer. Methods Fluids* 11 (1990) 189–207.
- [25] J. Ferziger, M. Peric, *Computational Methods for Fluid Dynamics*, Springer, Berlin, 1996.